Colloids and Surfaces B: Biointerfaces 194 (2020) 111209

Contents lists available at ScienceDirect

Colloids and Surfaces B: Biointerfaces

journal homepage: www.elsevier.com/locate/colsurfb

Solid lipid nanoparticles-mediated enhanced antidepressant activity of duloxetine in lipopolysaccharide-induced depressive model

Isra Rana[a], Namrah Khan[a], Muhammad Mohsin Ansari[a], Fawad Ali Shah[a], Fakhar ud Din[b], Sadia Sarwar[a], Muhammad Imran[a], Omer Salman Qureshi[c], Ho-Ik Choi[d], Cheol-Ho Lee[d], Jin-Ki Kim[d,**], Alam Zeb[a,*]

[a] Riphah Institute of Pharmaceutical Sciences, Riphah International University, Islamabad, Pakistan
[b] Department of Pharmacy, Quaid-i-Azam University, Islamabad, Pakistan
[c] Department of Pharmacy, Forman Christian College, Lahore, Pakistan
[d] College of Pharmacy, Institute of Pharmaceutical Science and Technology, Hanyang University, Ansan, Gyeonggi, Republic of Korea

ARTICLE INFO

Keywords:
Duloxetine
Antidepressant activity
Solid lipid nanoparticles
Lipopolysaccharide-induced depression
Brain-derived neurotropic factor

ABSTRACT

The potential of duloxetine-loaded solid lipid nanoparticles (DLX-SLNs) for enhanced antidepressant activity was investigated in the current study. Nano-template engineering technology was successfully employed for the preparation of DLX-SLNs. *In vivo* forced swim and tail suspension tests were used to evaluate behavioral changes of rats in lipopolysaccharide-induced depression. The determination of brain-derived neurotropic factor (BDNF) in brain and plasma was carried out using enzyme-linked immunosorbent assay. The incorporation efficiency of optimized DLX-SLNs formulation was found to be 80 % with particle size of 114.5 nm, PDI of 0.29 and zeta potential of -18.2 mV. Powder X-ray diffractometry and differential scanning calorimetry demonstrated sufficient incorporation into lipid matrix and amorphous behavior of DLX. *In vitro* release profile of DLX-SLNs showed a sustained release achieving a cumulative amount of 52.97 % for 24 h. DLX-SLNs showed a significant decrease in immobility time in forced swim and tail suspension tests. DLX-SLNs increased BDNF levels in plasma and brain after 2 weeks. Immunohistochemistry results demonstrated significant reduction in the expression of tumor necrosis factor-α and cyclooxygenase enzyme-2 in brain. In conclusion, solid lipid nanoparticles can be utilized as a potential carrier for the delivery of antidepressant drugs into the brain.

1. Introduction

Depression is a devastating mental illness affecting the behavioral, psychological and physical health and resulting in major social and economic implications [1]. It has been reported that about 264 million people suffer from depression worldwide [2]. Depression is associated with significantly impaired social interaction and quality of life, increased suicidal thoughts, higher risk of developing heart diseases, and increased morbidity and mortality [3,4]. The pathophysiology of depression is complex and poorly understood, and a number of hypotheses have been suggested to provide the basis of depression involving imbalance in cytokines and neurotrophins levels [5,6]. Duloxetine (DLX), a first line treatment of depression, acts *via* dual inhibition of serotonin and norepinephrine reuptake [7]. It has also been utilized for anxiety disorders, fibromyalgia and peripheral neuropathies associated to diabetes [8,9]. DLX is preferred over other antidepressant drugs for its better efficacy and tolerability, quicker recovery, dual inhibition property, fewer side effects, ability to treat both emotional and physical symptoms and lower affinity for other neuronal receptors [10,11]. However, poor aqueous solubility (~130 μg/mL at 25 °C), extensive metabolism by hepatic enzymes and its susceptibility to degradation at acidic pH cause low (~50 %), variable and dissolution-rate dependent oral bioavailability of DLX [12]. Moreover, the presence of blood-brain barrier (BBB) hampers the access of antidepressant drugs into the brain following oral and parenteral administration, thereby making treatment more challenging. BBB is composed of tightly bound endothelial cells and a number of pericytes, astroglia and mast cells to render brain impermeable for overwhelming majority of large and small molecules [13]. The expression of efflux pumps (mainly P-gps and MRPs) on the apical surface of brain endothelial cells hinder the transcellular

* Corresponding author at: Riphah Institute of Pharmaceutical Science, Riphah International University, Sector G-7/4, 7th Avenue, Islamabad 44000, Pakistan.
** Corresponding author at: College of Pharmacy, Institute of Pharmaceutical Sciences and Technology, Hanyang University, 55 Hanyangdaehak-ro, Sangnok-gu, Ansan, Gyeonggi 15588, Republic of Korea.
E-mail addresses: jinkikim@hanyang.ac.kr (J.-K. Kim), alam.zeb@riphah.edu.pk (A. Zeb).

https://doi.org/10.1016/j.colsurfb.2020.111209
Received 5 May 2020; Received in revised form 16 June 2020; Accepted 19 June 2020
Available online 21 June 2020

transport of drugs across the BBB [13,14]. These formidable obstacles often restrict the effective brain delivery and optimal therapeutic response of antidepressant drugs.

Formulation approaches including the use of mesoporous silica [15], microemulsion [16] and lipid nanoparticles [17] have been utilized to overcome low aqueous solubility, dissolution and oral bioavailability of DLX. In another study, nanostructured lipid carriers were utilized to improve the poor brain delivery of DLX *via* intranasal administration [18]. However, none of the previously reported studies investigated the *in vivo* antidepressant effects of DLX-loaded solid lipid nanoparticles (DLX-SLNs) after parenteral administration. SLNs are the first generation of lipid nanoparticles composed of solid lipid core covered by a surfactant shell to stabilize the system [19]. SLNs are preferred over their colloidal counterparts due to a number of advantages including biocompatibility, high drug incorporation, sustained drug release, improved physical and chemical stabilities, enhanced drug protection in physiological environment, improved bioavailability and convenient large scale production [20,21]. More importantly, owing to their small particle size and lipid nature, SLNs have the inherent ability to penetrate the BBB even without any surface functionalization [22]. Considering their favorable attributes, SLNs could be a promising drug delivery system for improving the brain delivery of DLX.

The current study is intended to evaluate the *in vivo* antidepressant potential of DLX-SLNs in the experimental animal models. DLX-SLNs were prepared and optimized by nano-template engineering technique using stearyl alcohol as a solid lipid and a mixture of Poloxamer 188 and Tween 80 as a surfactant shell, followed by physicochemical characterization and *in vitro* release studies. The *in vivo* antidepressant effects of DLX-SLNs were evaluated by behavioral tests in lipopolysaccharide (LPS)-induced depressive animal model. The molecular markers of depression were assessed by using enzyme-linked immunosorbent assay (ELISA) to determine the concentration of brain-derived neurotropic factor (BDNF) in brain and plasma, and immunohistochemistry to measure the expression of tumor necrosis factor-α (TNF-α) and cyclooxygenase enzyme-2 (COX-2) in brain.

2. Materials and methods

2.1. Materials

Duloxetine (DLX) was kindly gifted by Vision Pharmaceuticals, Islamabad, Pakistan. Lipopolysaccharide (LPS, from *Escherichia coli*), stearyl alcohol, Tween 80 and Poloxamer 188 were obtained from Sigma Aldrich (St. Louis, MO, USA). All other chemicals utilized in the study were of analytical grade and used without further purification.

2.2. Preparation of DLX-SLNs

Nano-template engineering technique was employed with slight modifications for the preparation of DLX-SLNs [23,24]. Momentarily, stearyl alcohol was melted in a water bath at 75 °C followed by the addition of Poloxamer 188, Tween 80 and DLX. Filtered deionized water maintained at 75 °C was then added to the molten lipid/surfactant mixture with constant magnetic stirring at 1600 rpm for 30 min to form a clear nano-emulsion. Finally, DLX-SLNs were obtained by rapidly cooling down the nano-emulsion at 4 °C in ice bath. The unloaded drug and large aggregates were removed from DLX-SLNs by filtering the formulation with a 0.45 μm PVDF syringe filter and subsequently stored at 4 °C until further analysis. The composition of DLX-SLNs with different lipid to surfactants ratio is presented in Table 1.

2.3. Determination of particle size, polydispersity index, zeta potential and incorporation efficiency

DLX-SLNs were characterized for the average particle size, polydispersity index (PDI), zeta potential and drug incorporation efficiency. For this purpose, DLX-SLNs were suitably diluted with filtered deionized water and their particle size, PDI and zeta potential were determined by using photon correlation spectroscopy and electrophoretic light scattering technique, respectively, with a Zetasizer ZS 90 (Malvern Instruments, Malvern, Worcestershire, UK). To determine the drug incorporation efficiency and loading content, DLX-SLNs freed from unloaded DLX were dissolved in methanol followed by drug content analysis with a UV–vis spectrophotometer at 288 nm (V-530; JASCO Corporation, Tokyo, Japan). The possibility of absorption from the ingredients other than DLX (stearyl alcohol, Poloxamer 188 and Tween 80) was excluded by measuring absorbance of stearyl alcohol, Poloxamer 188, Tween 80 and blank SLNs at 288 nm along with their UV spectra between 200 − 400 nm and subsequently comparing them to those of DLX (supplementary material). The calculations for incorporation efficiency and loading content were made by using the following equations.

$$\text{Incorporation efficiency}\,(\%) = \frac{\text{weight of DLX in DLX-SLNs}}{\text{total weight of DLX added}} \times 100$$

$$\text{Loading content}\,(\%) = \frac{\text{weight of DLX in DLX-SLNs}}{\text{total weight of DLX-SLNs}} \times 100$$

The storage stability of optimized DLX-SLNs formulation was evaluated for 8 weeks at 4 °C. For this purpose, DLX-SLNs were stored at 4 °C in dry and sealed glass vials flushed with a stream of nitrogen gas. Samples were subsequently collected at 1, 2, 4, 6 and 8 weeks and monitored for changes in particle size, PDI, zeta potential, incorporation efficiency and loading content.

2.4. Transmission electron microscopy (TEM)

The morphological features of the optimized DLX-SLNs were assessed with field-emission transmission electron microscopy (JEM-2100 F; JEOL, Tokyo, Japan). Diluted DLX-SLNs were permitted to adsorb on to a 400-mesh carbon-coated copper grid followed by adding a drop of 1% phosphotungstic acid aqueous solution for negative staining and drying at ambient temperature. The DLX-SLNs were finally imaged with a TEM at an accelerating voltage of 200 kV [19].

2.5. Differential scanning calorimetry (DSC)

Thermal analysis of lyophilized DLX-SLNs and their individual solid components (DLX, stearyl alcohol and Poloxamer 188) was performed by using a differential scanning calorimeter (DSC Q20; TA Instrument, New Castle, DE, USA). DLX-SLNs were lyophilized using a freeze-dryer (TFD5503, Ilshin Biobase Co., Ltd. Gyeonggido, Republic of Korea) without a cryoprotectant to avoid its interrupting peaks in the solid state characterization. For DSC analysis, samples (5 − 10 mg) were melted in aluminum pans over a heating rang of 0 − 250 °C increased at a rate of 10 °C/min.

2.6. Powder X-ray diffractometry (PXRD)

The crystalline behavior of lyophilized DLX-SLNs and their individual solid components (DLX, stearyl alcohol and Poloxamer 188) was investigated by using a powder X-ray diffractometer (D8 Advance-Bruker, Billerica, MA, USA). For this purpose, samples were scanned over 2θ range of 3°-70° at a rate of 0.02°/s, with a 40 mA current and 40 kV voltage [25].

2.7. Fourier transform infrared spectroscopy (FTIR)

The molecular vibrations of lyophilized DLX-SLNs and their individual solid components (DLX, stearyl alcohol and Poloxamer 188) were monitored with an attenuated total reflectance Fourier transform

Table 1
Composition and physicochemical properties of DLX-SLNs.

Composition (mg)					Physiochemical properties				
Formulation	**SA**	**P 188**	**Tw 80**	**DLX**	**PS (nm)**	**PDI**	**ZP (mV)**	**IE (%)**	**LC (%)**
F1	10	2.5	35	5.0	463 ± 8.3	0.80 ± 0.23	−14.0 ± 0.8	81.0 ± 1.2	7.7 ± 0.1
F2	10	5.0	50	5.0	219 ± 3.9	0.40 ± 0.02	−10.0 ± 1.1	82.0 ± 2.2	5.9 ± 0.2
F3	**10**	**7.5**	**40**	**5.0**	**114.5 ± 2.0**	**0.29 ± 0.03**	**−18.2 ± 1.8**	**80.0 ± 4.16**	**6.4 ± 0.3**
F4	10	7.5	30	5.0	177 ± 1.3	0.25 ± 0.40	−16.0 ± 0.9	87.0 ± 3.2	8.3 ± 0.3
Blank	**10**	**7.5**	**40**	–	**103 ± 2.1**	**0.12 ± 0.09**	**−12.4 ± 1.3**	–	–

SA; stearyl alcohol, P 188; Poloxamer 188, Tw 80; Tween 80, DLX; duloxetine, PS; particle size, PDI; polydispersity index, ZP; zeta potential, IE; incorporation efficiency, LC; loading content.
Data are expressed as the mean ± S.D. (n = 3).

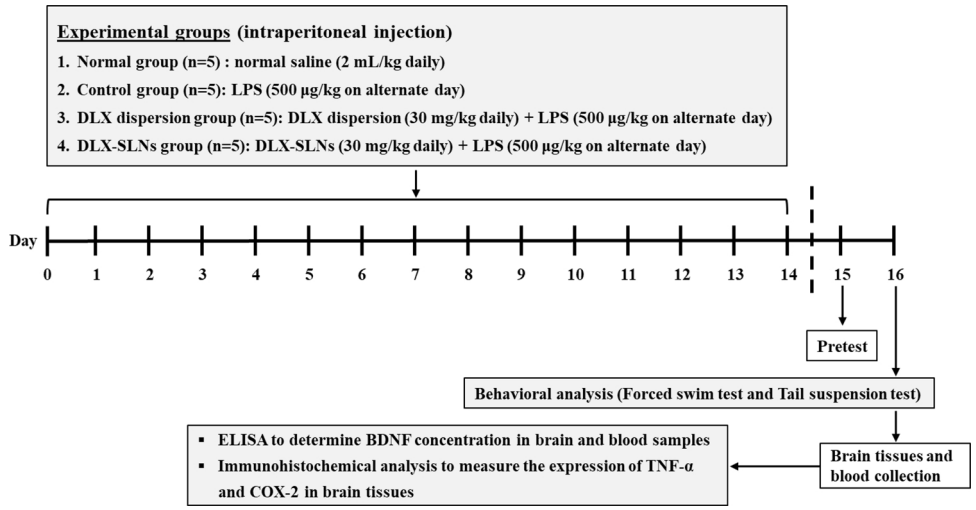

Fig. 1. Diagrammatic illustration of *in vivo* study design showing experimental groups, number of animals, treatment schedule and analysis performed in LPS-induced depressive-like model.

infrared spectrophotometer (Eco Alpha II- Bruker, Billerica, MA, USA). The samples were placed on a diamond ATR crystal and infrared transmission spectra were recorded over the wave number range of $4000-400\,cm^{-1}$ at a resolution of $4\,cm^{-1}$.

2.8. In vitro release study

The dialysis membrane diffusion technique was used to investigate the *in vitro* release of DLX from DLX-SLNs with phosphate buffer saline (PBS, pH 7.4) as a release medium [23]. DLX-SLNs or DLX dispersion (equivalent to 5 mg of DLX) was added to a presoaked dialysis membrane having molecular cut-off weight of 3500 Da (Spectrum Laboratories, Inc., Rancho Dominguez, CA, USA). The dialysis membranes were submerged in 500 mL of the release medium supplemented with 0.1 % Tween 80 as a solubilizing agent, and maintained at 37 ± 0.5 °C with constant stirring at 100 rpm. At predetermined time intervals, an aliquot of 2 mL was obtained from the release medium for 24 h and analyzed with a UV–vis spectrophotometer at 288 nm to determine the amount of DLX released. The total volume of the release medium was kept constant throughout the experiment by instantly replenishing with same amount of PBS after obtaining the samples.

2.9. In vivo antidepressant activity of DLX-SLNs

2.9.1. Animals

The *in vivo* antidepressant activity of DLX-SLNs was investigated in male Sprague Dawley rats (200 ± 20 g) obtained from the National Institute of Health (Islamabad, Pakistan). The study animals were provided with sufficient food and water and acclimatized with the standard laboratory environment having temperature and relative humidity maintained at 25 ± 0.5 °C and 40–60 %, respectively. All experimental protocols on animals were in line with the NIH policy and animal welfare act, and were duly approved by the Institutional Research and Ethics Committee of Riphah Institute of Pharmaceutical Sciences.

2.9.2. Experimental design

The antidepressant activity of DLX-SLNs was evaluated in LPS-induced depressive-like animal model [26]. For this purpose, rats were randomly divided into four groups (n = 5) including normal group (was not challenged with LPS and received normal saline), control group (challenged with LPS and did not receive any treatment), DLX dispersion group (challenged with LPS and treated with DLX dispersion) and DLX-SLNs group (challenged with LPS and treated with DLX-SLNs). Normal saline at a dose of 2 mL/kg and DLX dispersion or DLX-SLNs at a dose equivalent to 30 mg/kg of DLX were administered to respective groups by a daily intraperitoneal injection for 14 days. Additionally, rats in control, DLX dispersion and DLX-SLNs groups received LPS (500 µg/kg) on alternate day for a period of 14 days. The animals were subjected to a pretest and behavioral analysis on day 15 and 16, respectively. Blood samples were then collected from rats *via* cardiac puncture and centrifuged at 3000 *g* for 15 min to separate plasma. After blood collection, each rat was sacrificed and brain was removed by decapitation and rinsed with normal saline. Plasma and brain samples were stored at -30 °C until further analysis. The diagrammatic illustration of experimental design in LPS-induced depressive-like model is shown in Fig. 1.

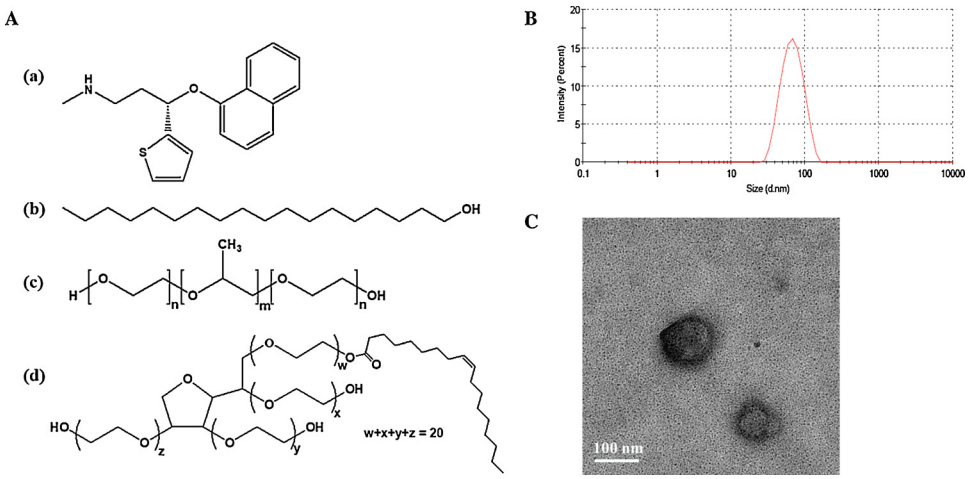

Fig. 2. Chemical structures (A) of DLX (a), stearyl alcohol (b), Poloxamer 188 (c) and Tween 80 (d), particle size distribution curve (B) and TEM image (C) of DLX-SLNs.

2.9.3. Behavioral analysis

The behavioral analysis of rats was conducted by using forced swim and tail suspension tests. Forced swim test was performed in a glass cylinder (21 × 21 × 50 cm) filled with water up to 35 cm and maintained at 24 ± 1 °C [27]. Each rat was subjected to a pretest by placing it in the cylinder for 15 min and then allowed to dry at room temperature. On the next day, each rat was placed again in the cylinder for 5 min under the same conditions and immobility time was measured. Immobility was marked by the absence of movement to escape and float in water or making efforts other than those to keep its head above water level. Water was changed after each swim to avoid behavioral changes due to contamination.

Tail suspension test was performed by suspending the rat by its tail using adhesive tape thereby holding it 50 cm above the ground [28]. Climb stopper was placed around the tail to prevent rat from grabbing onto its tail. Immobility time, characterized by the absence of escape behavior, was measured for each rat over a period of 6 min.

2.9.4. Quantification of BDNF concentrations in plasma and brain samples

The concentration of BDNF in plasma and brain samples obtained from rats after behavioral studies was determined by ELISA. For this purpose, cortices were separated from brain samples, homogenized with PBS, centrifuged at 3000 *g* for 15 min and supernatant was collected. Finally, BDNF concentration in plasma and brain supernatant was determined by using its respective rat ELISA kit (Elabscience, Wuhan, Hubei, China), according to the manufacturer's instructions.

2.9.5. Immunohistochemical evaluation

For measuring the expression of TNF-α and COX-2 by immunohistochemistry, brain tissues from separate rats (n = 5 for each group) were isolated and kept in 4% paraformaldehyde solution for fixation. The preserved brain tissues were embedded in paraffin, sliced into 5 µm sections and mounted on the slides. Brain sections were then deparaffinized with xylene and rehydrated with a series of ethanol concentrations (100, 90, 80 and 70 %) followed by washing with distilled water and PBS. Antigen retrieval was performed with protein kinase and incubated in hydrogen peroxide. The sections were subsequently blocked by using 5% serum and incubated overnight with respective primary antibody. After 12 h, the slides were treated with the secondary antibody for 2 h and then with ABC reagents (Standard Vectastain ABC Elite Kit; Vector Laboratories, Burlingame, CA, USA) for 1 h at ambient temperature. The slides were subsequently washed with PBS and stained with 3, 3′-Diaminobenzidine tetrahydrochloride solution followed by washing distilled water, dehydrating with a series of ethanol concentrations (70, 90 and 100 %) and fixing in xylene. The slides were finally cover-slipped with mounting media and observed under light microscope (Olympus Corporation, Tokyo, Japan) connected to digital photomicroscopy system. Images were captured and visually observed for the expression of TNF-α and COX-2. The expression of TNF-α and COX-2 in the cortical region of brain was quantified with ImageJ software by analyzing the images adjusted to their threshold intensities. The relative integrated density of each sample was determined relative to normal [29].

2.10. Statistical analysis

All the experiments included in this study were performed at least in triplicate and results are displayed as the mean ± standard deviation (S.D.). Student's *t*-test was applied to calculate statistical significance among the groups at the probability level of p less than 0.05 by using SPSS software (SPSS Inc., Chicago, IL, USA).

3. Results

3.1. Optimization and physicochemical properties of DLX-SLNs

In this study, DLX-SLNs were successfully prepared by using a well-known nano-template engineering technique and optimized with different ratios of stearyl alcohol as a solid lipid and Poloxamer 188 and Tween 80 as a surfactant mixture. The chemical structures of DLX, stearyl alcohol, Poloxamer 188 and Tween 80 are presented in Fig. 2A. The amount of stearyl alcohol and DLX was fixed at 10 and 5 mg, respectively. On the other hand, Poloxamer 188 and Tween 80 ratios were varied as 2.5/35, 5/50, 7.5/40 and 7.5/30 (w/w) to produce a stabilizing layer with hydrophilic-lipophilic balance (HLB) values of 15.9, 16.2, 17.2 and 17.8, respectively. The composition and physicochemical properties of DLX-SLNs are presented in Table 1. DLX-SLNs were optimized on the basis of average particle size, PDI, zeta potential and incorporation efficiency. Particle size and PDI of DLX-SLNs substantially decreased (463 nm and 0.8 *vs.* 114.5 nm and 0.29), and zeta potential increased (-14 *vs.* -18.2 mV) as the HLB value of the system increased from 15.9 to –17.2. Further increase in the HLB value of DLX-SLNs to 17.8 (F4) resulted in an increase in their particle size up to 177 nm, accompanied by an increase in the incorporation efficiency (87 %). Despite of the slightly higher incorporation efficiency at HLB of 17.8 (F4), DLX-SLNs with HLB value of 17.2 (F3) was selected as an optimized formulation due to its optimal particle size, PDI, surface charge and sufficient incorporation efficiency. The optimized formulation, F3, with stearyl alcohol/Poloxamer 188/Tween 80/DLX with 10/7.5/40/5 ratio (w/w) was therefore evaluated for physicochemical

Table 2
Storage stability of DLX-SLNs for 8 weeks at 4 °C.

Week	Particle size (nm)	PDI	Zeta potential (mV)	Incorporation efficiency (%)	Loading content (%)
0	114.5 ± 2.0	0.29 ± 0.03	−18.2 ± 1.8	80.0 ± 4.2	6.4 ± 0.3
1	113.3 ± 3.7	0.28 ± 0.03	−18.5 ± 1.2	79.8 ± 3.5	6.4 ± 0.3
2	114.9 ± 4.8	0.28 ± 0.02	−18.3 ± 0.9	79.2 ± 5.1	6.3 ± 0.4
4	116.8 ± 5.2	0.29 ± 0.03	−18.1 ± 1.4	78.7 ± 4.3	6.3 ± 0.3
6	117.5 ± 4.1	0.28 ± 0.01	−17.8 ± 2.1	78.4 ± 4.9	6.3 ± 0.4
8	119.1 ± 6.7	0.30 ± 0.02	−17.9 ± 0.8	77.6 ± 3.7	6.2 ± 0.3

Data are expressed as the mean ± S.D. (n = 3).

properties, *in vitro* drug release and *in vivo* antidepressant activity.

The physicochemical characteristics of nanoparticles play a vital role in the efficient brain delivery by affecting their ability to penetrate the BBB. The optimized DLX-SLNs formulation (F3) displayed nanometric particle size of 114.5 nm accompanied with a low PDI value (0.29) and a unimodal particle size distribution curve (Fig. 2B). In addition, DLX-SLNs exhibited negatively charged surface as indicated by the zeta potential value of -18.2 mV. DLX-SLNs showed high drug incorporation efficiency and loading content of 80 % and 6.4 %, respectively. TEM image of the optimized DLX-SLNs revealed spherical and uniform shape with smooth surface morphology (Fig. 2C). TEM image of DLX-SLNs also showed a particle size of around 100 nm, consistent with the results of photon correlation spectroscopy. Taken together, DLX-SLNs possessed optimum physicochemical properties required for nano-formulations and efficient brain delivery. Furthermore, stability of the optimized DLX-SLNs was assessed by measuring changes in the physicochemical properties for 8 weeks after storage at refrigerator condition (4 °C). DLX-SLNs retained their physicochemical properties as no significant changes were observed in particle size, PDI, zeta potential, incorporation efficiency and loading content for 8 weeks (Table 2). These results demonstrated excellent storage stability of DLX-SLNs for 8 weeks at 4 °C.

3.2. Solid state characterization of DLX-SLNs

The thermal phase transitions of lyophilized DLX-SLNs, blank SLNs and their individual solid ingredients were monitored by DSC to investigate polymorphic changes and DLX-lipid interaction. DSC curves of DLX (a), stearyl alcohol (b) and Poloxamer 188 (c) exhibited sharp endothermic peaks about 171.8 °C, 60 °C and 56 °C at their respective melting temperatures (Fig. 3A). In contrary, thermal peaks of stearyl alcohol appeared at slightly lower temperatures between 46 − 50 °C in the thermograms of blank SLNs (d) and DLX-SLNs (e). Moreover, the sharp endothermic peak of DLX disappeared in DLX-SLNs (e).

The degree of crystallinity of lyophilized DLX-SLNs, blank SLNs and their solid ingredients were further investigated by PXRD (Fig. 3B). The diffractograms of DLX (a) displayed a number of distinct crystalline peaks at angles of 18.7°, 20.5°, 21.6° and 23.4°. Likewise, indicative crystalline peaks were demonstrated at 16.1°, 17.1°, 19.8° and 23.5° for stearyl alcohol (b), and at 19.3° and 23.5° for Poloxamer 188 (c). However, stearyl alcohol showed small humps (instead of sharp crystalline peaks) of reduced intensity between 20 − 22° in the PXRD patterns for blank SLNs (d) and DLX-SLNs (e). The characteristic peaks of DLX were also missing in the diffractogram of DLX-SLNs.

The molecular interactions of DLX with formulation ingredients in DLX-SLNs were studied with FTIR spectroscopy, and the results are presented in Fig. 3C. FTIR spectrum of DLX (a) revealed characteristic C—H stretch at 2965 cm^{-1}, C—O—C stretch at 1217 cm^{-1} and multiple peaks for aromatic groups (1577 – 1097 cm^{-1}). The distinct alcoholic (−OH) stretching vibration was observed at 3332 cm^{-1} along with peaks for long alkyl chain at 1472 and 1067 cm^{-1} in stearyl alcohol (b), while Poloxamer 188 (c) exhibited −OH stretching vibration at 2889 cm^{-1}. In contrary, the distinct DLX peaks were missing in FTIR spectra of blank SLNs (d) and DLX-SLNs (e). Collectively, the results of solid state characterization corresponded well with each other.

3.3. In vitro release of DLX from DLX-SLNs

The *in vitro* release of DLX from DLX-SLNs for 24 h is presented in Fig. 4. DLX release rate from DLX-SLNs was slightly fast for the initial 2 h (20.8 %) with a subsequent slow and sustained drug release reaching 52.9 % at 24 h. On the other hand, the DLX dispersion reached 94 % after 8 h with 51 % of DLX release within 2 h, indicating a much faster release than DLX-SLNs. In comparison, only 31.6 % drug release was observed from DLX-SLNs in 8 h. These results suggest the prolonged DLX release from DLX-SLNs without a prominent initial burst release.

3.4. Immobility time in behavioral despair tests

The immobility time was monitored as a measure of LPS-induced depressive behavior in rats and the effectiveness of DLX-SLNs. Immobility is a state of behavioral despair and used as an indicator of depression. The effects of DLX-SLNs treatment on immobility time in forced swim test are presented in Fig. 5A. The results indicated that DLX-SLNs substantially reduced the immobility time (143.4 ± 3.5 s) compared to control (210.6 ± 12.6 s) and DLX dispersion-treated rats (187.4 ± 4.8 s). The immobility time of DLX-SLNs group was comparable to that of rats in normal group (147.2 ± 12.3 s). Likewise, DLX-SLNs-treated rats exhibited significantly decreased immobility time (126.8 ± 5.3 s) in the tail suspension test in comparison with control (226.8 ± 3.0 s) and DLX dispersion-treated (157.4 ± 9.7 s) groups (Fig. 5B). The results of forced swim and tail suspension tests

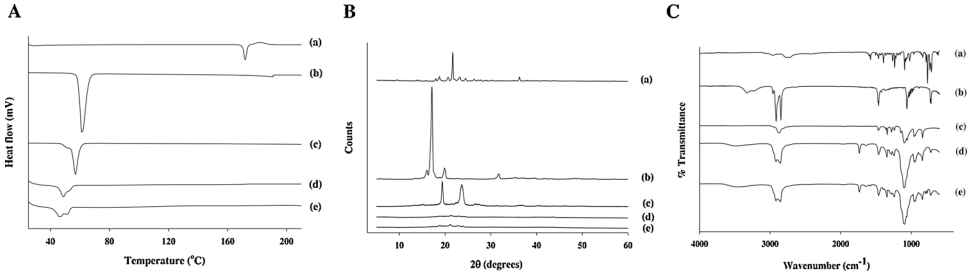

Fig. 3. DSC thermograms (A), PXRD diffractograms (B) and FTIR spectra (C) of DLX (a), stearyl alcohol (b), Poloxamer 188 (c), blank SLNs (d) and DLX-SLNs (e).

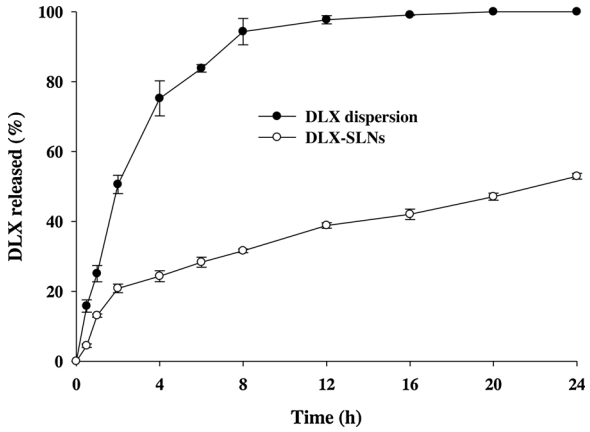

Fig. 4. *In vitro* release profiles of DLX-SLNs in phosphate buffer saline (pH 7.4) for 24 h at 37 °C. Data are expressed as the mean ± S.D. (n = 3).

suggest enhanced *in vivo* antidepressant activity of DLX-SLNs.

3.5. Effect of DLX-SLNs on BDNF concentrations

In vivo antidepressant activity of DLX-SLNs was further evaluated by measuring BDNF concentrations in plasma and prefrontal cortex. The results showed that chronic administration of LPS in control group significantly reduced BDNF concentration in plasma and brain compared to normal group. As shown in Fig. 6A, DLX-SLNs treatment resulted in 3.58- and 1.67-fold increase in plasma BDNF concentration (515.6 ± 39.7 pg/mL) compared to control (143.8 ± 10 pg/mL) and DLX dispersion (308.8 ± 5.9 pg/mL). The brain BDNF concentration of DLX-SLNs group (599.0 ± 91.6 pg/mL) was also 1.68- and 1.42-times higher than that of control (355.9 ± 25 pg/mL) and DLX dispersion-treated (428.8 ± 38.4 pg/mL) group, respectively (Fig. 6B). It is noteworthy to mention that plasma and brain BDNF concentrations after DLX-SLNs treatment were comparable to normal rats (599.7 ± 95.2 pg/mL in plasma and 646.1 ± 122.6 pg/mL in brain). From the results, DLX-SLNs successfully improved BDNF concentrations in LPS-induced depressive-like model. These findings are in consistent with those obtained in the behavioral despair tests.

3.6. Effects of DLX-SLNs on TNF-α and COX-2 expression in brain

The effects of DLX-SLNs-treatment on LPS-induced neuroinflammation were evaluated by determining the expression levels of TNF-α and COX-2 in brain. The immunohistochemical micrographs showed that LPS administration substantially increased the immunolabelling for TNF-α and COX-2 in brain tissues of control rats (Fig. 7A). DLX-SLNs attenuated immunopositivity for inflammatory factors, TNF-α and COX-2, in brain while control and DLX dispersion groups retained their immunopositivity. As presented in Fig. 7B and 7C, the relative integrated density of TNF-α and COX-2 in brain was also significantly reduced by DLX-SLNs (1.9 ± 0.5 and 2.6 ± 0.4) compared to control (7.8 ± 1 and 6.9 ± 0.6) and DLX dispersion (7.4 ± 1.2 and 6.6 ± 1). Similarly, DLX-SLNs reduced the number of cells expressing TNF-α and COX-2 in brain more efficiently than DLX dispersion (Table 3). From the results, the enhanced antidepressant activity of DLX-SLNs in LPS-induced depressive model was associated with a remarkable suppression of pro-inflammatory cytokines in the frontal cortex of brain.

4. Discussion

SLNs, comprised of a solid lipid core and a surfactant shell, have extensively been utilized to tune basic features of the incorporated drugs including their physicochemical properties and biological responses [21]. SLNs are well-tolerated *in vivo* since they are composed of biocompatible, biodegradable and non-toxic lipids, and surfactants of GRAS (generally regarded as safe) category such as Tween 80, Span 80 and Poloxamer 188. One of the key advantage of SLNs is their inherent ability to penetrate BBB because of their small particle size and lipophilic nature, which makes SLNs an ideal carrier for drug delivery into the brain [22]. In the current study, we developed DLX-SLNs and investigated their potential for enhanced *in vivo* antidepressant activity of DLX. Nano-template engineering technique was successfully utilized to prepare DLX-SLNs by using stearyl alcohol, Poloxamer 188 and Tween 80 as formulation ingredients. This particular technique involves the formation of o/w micro-emulsion which acts as a precursor and produce SLNs upon rapid cooling [30]. Stearyl alcohol, a saturated fatty alcohol containing 18 carbons with melting point of 59.8 °C, was used to form lipid core of DLX-SLNs. The lipid core with a melting point above body temperature has been reported to provide high incorporation efficiency and sustained drug release due to the firm hydrophobic interaction [23]. In addition, a combination of Poloxamer 188 and Tween 80 was used to form a miscible surfactant shell to stabilize the lipid core of DLX-SLNs. The cumulative HLB value of the surfactant system is an important factor to achieve optimal physicochemical properties of SLNs, with HLB of ≥ 15.5 being the most suitable to stabilize fatty alcohols lipid cores [19,31]. Therefore, the ratio of Poloxamer 188 and Tween 80 was changed to obtain HLB value between 15.5 − 18. DLX-SLNs with HLB of 17.2 (F3) exhibited optimal particle size (114.5 nm), PDI (0.29), zeta potential (-18.2 mV) and incorporation efficiency (80 %). The physicochemical properties of nanoparticles

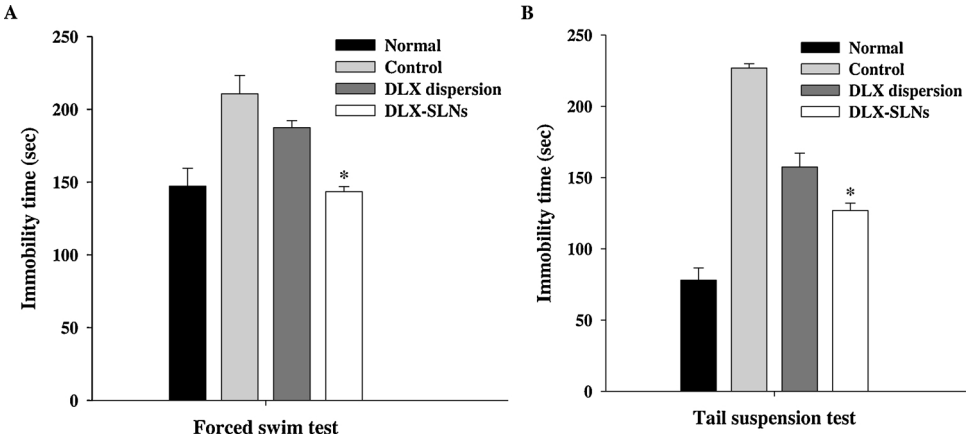

Fig. 5. Effects of DLX-SLNs on the immobility time in forced swim test (A) and tail suspension test (B) in LPS-induced depressive-like model. Data are expressed as the mean ± S.D. (n = 5). *p < 0.05 *versus* LPS control and DLX dispersion.

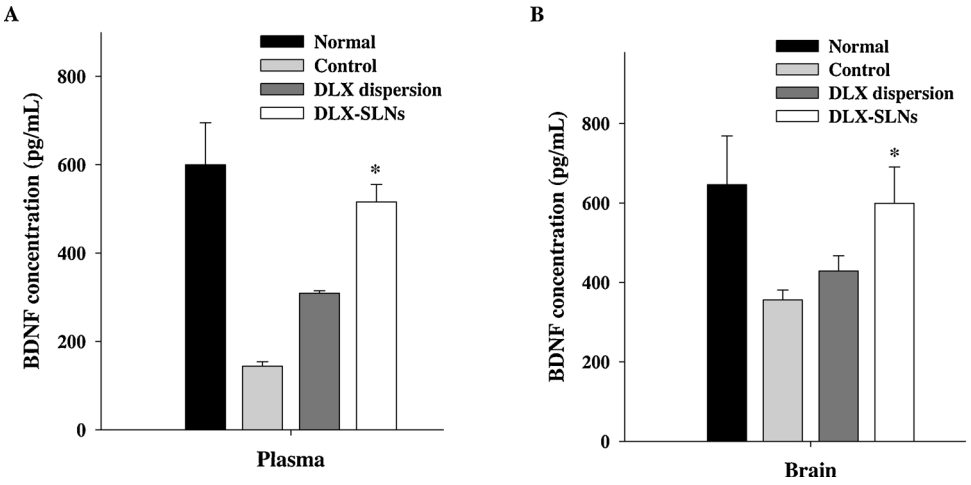

Fig. 6. BDNF concentrations in plasma (A) and brain (B) of normal, control, DLX dispersion and DLX-SLNs-treated rats. Data are expressed as the mean ± S.D. (n = 5). *p < 0.05 *versus* LPS control and DLX dispersion.

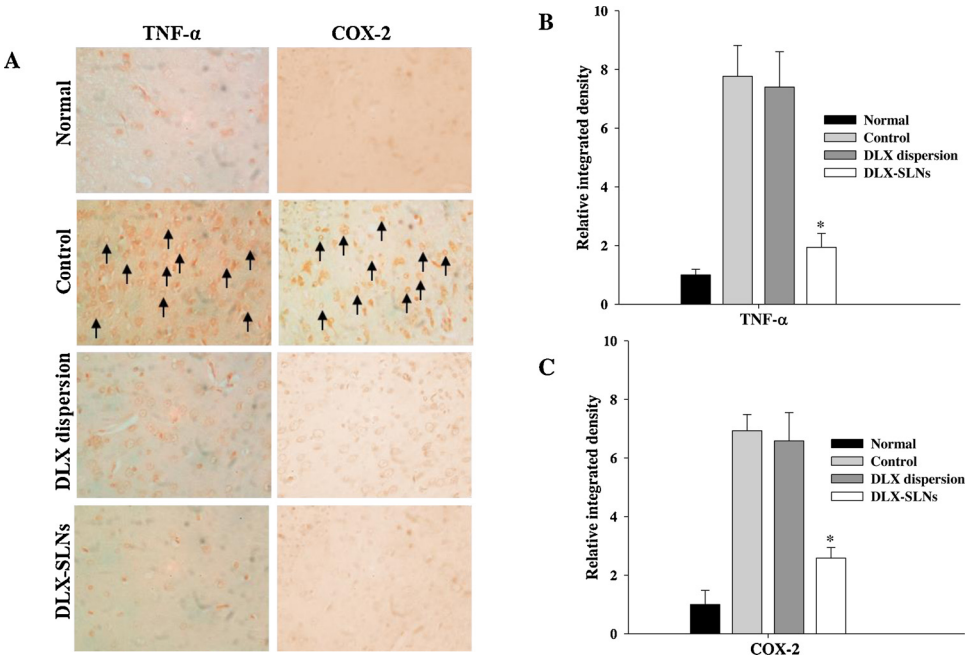

Fig. 7. Immunohistochemical micrographs of brain representing the expression of TNF-α and COX-2 (A), and the effects of DLX-SLNs on relative integrated density of TNF-α (B) and COX-2 (C) in brain. Arrows in the micrographs indicate positive immunostaining for TNF-α and COX-2. For relative integrated densities, data are expressed as the mean ± S.D. (n = 5). *p < 0.01 *versus* LPS control and DLX dispersion.

Table 3
Effects of DLX-SLNs on the number of cells expressing TNF-α and COX-2 in the brain of LPS-induced depressive-like rat model.

Group	Cell counts	
	TNF- α	COX-2
Normal	63.7 ± 12.1	72.3 ± 34.7
Control	494.3 ± 67.0	501.3 ± 39.8
DLX dispersion	471.0 ± 76.7	476.3 ± 69.5
DLX-SLNs	123.3 ± 30.0*	186.7 ± 26.2*

Data are expressed as the mean ± S.D. (n = 5). *p < 0.01 *versus* LPS control and DLX dispersion group.

have been demonstrated to greatly influence their brain delivery [32]. Nanoparticles with particle size of around 100 nm are the most desirable for enhancing permeability across the BBB [33]. The homogeneity of optimized DLX-SLNs was confirmed by a low PDI value and unimodal size distribution curve. Furthermore, negative zeta potential value (-18.2 mV) of DLX-SLNs and steric hindrance provided by Poloxamer 188 and Tween 80 would not only ensure colloidal stability, but also improve brain permeability without compromising the structural integrity of BBB [34]. DLX-SLNs exhibited adequately high incorporation efficiency to reduce the injection volume for intraperitoneal administration to rats in the experimental model. The storage temperature and formulation composition are important parameters to ensure the physical stability of SLNs as they affect particle growth, gelation tendency and drug retention [35,36]. The excellent storage stability of DLX-SLNs could be attributed to low refrigerator temperature (4 °C) together with electrostatic repulsion and steric stabilization imparted by Poloxamer 188 and Tween 80. It has been reported that higher temperatures and inadequate surface coverage by surfactant shell are detrimental for lipid nanoparticles stability [37]. The most common consequences of SLNs destabilization are increase in particle size and PDI, and reduction in zeta potential and drug incorporation efficiency. Higher storage temperature escalates the kinetic energy leading to increased collision between SLNs and decreased microviscosity with the resultant particle destabilization and aggregation [38,39]. The combined use of Poloxamer 188 and Tween 80 might also have contributed to the physical stability of DLX-SLNs. Surfactant mixture produces mixed films at the

interface with better surface coverage of lipid particles and increased viscosity thereby preventing fusion of film layers after particle collision [37,39]. Contribution from all these factors resulted in excellent storage stability of DLX-SLNs at 4 °C.

The incorporation efficiency and drug release behavior from SLNs are largely influenced by the phase transition of drug and lipid during preparation. As observed in DSC thermograms, sharp melting endotherms of individual DLX and stearyl alcohol indicated their crystalline nature. The conversion of native crystalline DLX to amorphous state and its complete solubilization in stearyl alcohol matrix resulted in the disappearance of DLX endothermic peak in DLX-SLNs [17]. Furthermore, the melting point of stearyl alcohol was reduced and melting range was broadened in blank SLNs and DLX-SLNs compared to bulk lipid. These changes in the melting endotherms could be ascribed to the less ordered crystal arrangement of lipid core in SLNs and small size effect, thereby requiring lower energy to melt than that of a perfect crystal lattice [40]. The loss of DLX crystallinity and reduction in the crystalline nature of stearyl alcohol matrix was also observed in PXRD patterns of DLX-SLNs, as evidenced by vanished DLX peak and diminished intensity of lipid peak. The successful incorporation of DLX into the stearyl alcohol core of DLX-SLNs was also supported by the FTIR spectra. In addition, no significant chemical interaction existed between the drug and formulation ingredients.

In vitro release profile of DLX-SLNs suggested a slow and sustained pattern, which has clinical significance in minimizing administration frequency and dose. Despite the relatively fast release rate in the initial 2 h, a profound "burst release" of DLX was not observed from DLX-SLNs. The initial fast release rate could be attributed to the diffusion of a small portion of loosely attached DLX at or near the surface of DLX-SLNs into release medium [41]. In the second phase of drug release, DLX-SLNs demonstrated a continuous and prolonged DLX release for 24 h which could be explained by immobilization of DLX in the lipid matrix due to strong hydrophobic interactions [42]. In addition to slow diffusion of DLX and gradual erosion of lipid core, hydrophilic surfactant shell of Poloxamer 188 and Tween 80 might also contribute to hinder drug release by serving as a mechanical barrier [43]. It is worth mentioning that the stearic stabilization effect of Poloxamer 188 could also play a crucial role in preventing rapid degradation of lipid matrix by lipolytic enzymes, thereby prolonging DLX release in physiological environment [43].

Our findings indicated enhanced *in vivo* antidepressant activity of DLX-SLNs in LPS-induced depressive model. LPS is widely utilized to induce depressive-like behavior in rodents characterized by cognitive impairment, decreased BDNF concentrations and elevated pro-inflammatory cytokines levels [5]. LPS-induced immobility in the inescapable circumstances of forced swim and tail suspension tests reflects behavioral despair, and reduction of immobility time by DLX-SLNs evidenced its superior antidepressant effects [44]. BDNF as a member of neurotrophic factors plays a crucial role in the neuronal survival, proliferation, differentiation and plasticity [45]. The clinical findings suggest that regulation of BDNF expression in brain could contribute to the pathophysiology and treatment of depression [6]. It has been reported that BDNF expression in the prefrontal cortex and its concentration in plasma is reduced in depressed patients [46,47]. Furthermore, a positive correlation has been found between plasma BDNF concentrations and brain BDNF levels in a number of animal species [48]. Our results demonstrated elevation in plasma and brain BDNF concentrations after treatment with DLX-SLNs, thereby improving behavioral functions by stabilizing neuronal plasticity. Our findings are consistent with the previous reports where repeated DLX administration increased BDNF levels in rats [45]. DLX-SLNs exhibited a substantial reduction in the expression of inflammatory parameters which could be linked to decreased depression. Growing evidence suggests the association of depression with increased oxidative stress and increased inflammatory responses [49,50]. It has been reported that exposure to stressful stimuli or LPS administration result in the activation of peripheral immune system to release cytokines. These cytokines are transported to brain, stimulating astrocytes and microglial cells which consequently secrete multiple pro-inflammatory mediators leading to neuroinflammation and depressive symptoms [5,51,52]. Increased levels of pro-inflammatory cytokines contribute to the pathogenesis of depression by interacting with neuroendocrine function, neurotransmitter metabolism, neural plasticity and behavior [53]. Studies have shown that depressed patients exhibit prominent features of inflammation characterized by raised levels of inflammatory markers such as TNF-α and COX-2 [54,55]. Furthermore, antidepressant drugs have been reported to reduce LPS-induced production of inflammatory parameters [56]. Taken together, our findings suggest improved antidepressant activity in LPS-induced depressive-like model which could be ascribed to the effective brain delivery mediated by DLX-SLNs.

Lipid-based nanoparticles improve brain delivery of drugs by a number of mechanisms which could explain the enhanced *in vivo* antidepressant activity of DLX-SLNs. Small particle size, lipophilicity and large surface area enable SLNs to efficiently deliver the incorporated drug to the brain by increasing their contact time and drug concentration at the BBB surface [24,57]. SLNs could also enhance drug transport across BBB by facilitating the processes of endocytosis, transcytosis and opening of endothelial tight junctions [33,58]. In addition, it has been reported that Tween 80 and Poloxamer 188 assist nanoparticles in crossing BBB by adsorbing lipoproteins from blood thereby facilitating receptor-mediated transport into the brain [59]. The inhibition of efflux transport system (particularly P-gp) and membrane fluidization because of surfactant shell in SLNs also play a role in improving drug transport across BBB [60]. The combining effects of these mechanisms might be attributed to enhanced therapeutic performance of DLX-SLNs in LPS-induced depressive model.

5. Conclusion

In this study, *in vivo* antidepressant activity of DLX-SLNs was investigated to reflect their true therapeutic potential in the animal model. DLX-SLNs significantly reduced depressive behavior in rats coupled with increased BDNF concentration in plasma and brain compared to DLX dispersion. The inflammatory markers of depression were also substantially suppressed by DLX-SLNs. These results suggest that DLX-SLNs could be a promising delivery system for effective brain delivery of DLX to treat depression, while avoiding the drawbacks of conventional formulations.

CRediT authorship contribution statement

Isra Rana: Conceptualization, Data curation, Formal analysis, Investigation, Methodology, Writing - original draft, Writing - review & editing. **Namrah Khan:** Conceptualization, Formal analysis, Writing - review & editing. **Muhammad Mohsin Ansari:** Data curation, Supervision, Resources, Software, Writing - review & editing. **Fawad Ali Shah:** Conceptualization, Data curation, Writing -review & editing. **Fakhar ud Din:** Data curation, Methodology, Writing - review & editing. **Sadia Sarwar:** Investigation, Writing - review & editing. **Muhammad Imran:** Formal analysis, Writing - review & editing. **Omer Salman Qureshi:** Investigation, Methodology, Writing - review & editing. **Ho-Ik Choi:** Investigation, Methodology, Writing - review & editing. **Cheol-Ho Lee:** Investigation, Methodology, Writing - review & editing. **Jin-Ki Kim:** Funding, Project administration, Supervision, Resources, Software, Writing - original draft, Writing - review & editing. **Alam Zeb:** Funding, Project administration, Supervision, Resources, Software, Writing - original draft, Writing - review & editing.

Declaration of Competing Interest

It is to confirm that the authors report no conflict of interest in the work.

Acknowledgements

The authors acknowledge the financial support of the Higher Education Commission of Pakistan (grant No: 21-1590/SRGP/R&D/HEC/2017) and the National Research Foundation of Korea (NRF) funded by the Ministry of Science and ICT (NRF-2017R1A2B4006458). Riphah Academy of Research and Education is also acknowledged for partial support through seed money grant program of Riphah International University.

Appendix A. Supplementary data

Supplementary material related to this article can be found, in the online version, at doi:https://doi.org/10.1016/j.colsurfb.2020.111209.

References

[1] J.F. Cryan, A. Markou, I. Lucki, Assessing antidepressant activity in rodents: recent developments and future needs, Trends Pharmacol. Sci. 23 (2002) 238–245.
[2] WHO, Depression Fact Sheet, (2020) Available from: https://www.who.int/news-room/fact-sheets/detail/depression . [Accessed 22-03-2020].
[3] C. Kiyohara, K. Yoshimasu, Molecular epidemiology of major depressive disorder, Environ. Health Prev. Med. 14 (2009) 71–87.
[4] F. Seligman, C.B. Nemeroff, The interface of depression and cardiovascular disease: therapeutic implications, Ann. N. Y. Acad. Sci. 1345 (2015) 25–35.
[5] A.H. Miller, V. Maletic, C.L. Raison, Inflammation and its discontents: the role of cytokines in the pathophysiology of major depression, Biol. Psychiatry 65 (2009) 732–741.
[6] Y. Shirayama, A.C. Chen, S. Nakagawa, D.S. Russell, R.S. Duman, Brain-derived neurotrophic factor produces antidepressant effects in behavioral models of depression, J. Neurosci. 22 (2002) 3251–3261.
[7] D.J. Goldstein, C. Mallinckrodt, Y. Lu, M.A. Demitrack, Duloxetine in the treatment of major depressive disorder: a double-blind clinical trial, J. Clin. Psychiatry 63 (2002) 225–231.
[8] A. Wright, C. Vandenberg, Duloxetine in the treatment of generalized anxiety disorder, Int. J. Gen. Med. 2 (2009) 153–162.
[9] M.P. Lunn, R.A. Hughes, P.J. Wiffen, Duloxetine for treating painful neuropathy, chronic pain or fibromyalgia, Cochrane Database Syst. Rev. (2014) Cd007115.
[10] J.E. Turcotte, G. Debonnel, C. de Montigny, C. Hebert, P. Blier, Assessment of the serotonin and norepinephrine reuptake blocking properties of duloxetine in healthy subjects, Neuropsychopharmacol. 24 (2001) 511–521.
[11] A. Sharma, M.J. Goldberg, B.J. Cerimele, Pharmacokinetics and safety of duloxetine, a dual-serotonin and norepinephrine reuptake inhibitor, J. Clin. Pharmacol. 40 (2000) 161–167.
[12] R.J. Lantz, T.A. Gillespie, T.J. Rash, F. Kuo, M. Skinner, H.Y. Kuan, M.P. Knadler, Metabolism, excretion, and pharmacokinetics of duloxetine in healthy human subjects, Drug Metab. Dispos. 31 (2003) 1142–1150.
[13] R. Gabathuler, Approaches to transport therapeutic drugs across the blood–brain barrier to treat brain diseases, Neurobiol. Dis. 37 (2010) 48–57.
[14] F.E. O'Brien, T.G. Dinan, B.T. Griffin, J.F. Cryan, Interactions between antidepressants and P-glycoprotein at the blood-brain barrier: clinical significance of in vitro and in vivo findings, Br. J. Pharmacol. 165 (2012) 289–312.
[15] M. Ganesh, P. Hemalatha, P.M. Mei, K. Rajasekar, H.T. Jang, A new fluoride mediated synthesis of mesoporous silica and their usefulness in controlled delivery of duloxetine hydrochloride a serotonin re-uptake inhibitor, J. Ind. Eng. Chem. 18 (2012) 684–689.
[16] P. Sindhu, S. Kumar, B. Iqbal, J. Ali, S. Baboota, Duloxetine loaded-microemulsion system to improve behavioral activities by upregulating serotonin and norepinephrine in brain for the treatment of depression, J. Psychiatr. Res. 99 (2018) 83–95.
[17] K. Patel, S. Padhye, M. Nagarsenker, Duloxetine HCl lipid nanoparticles: preparation, characterization, and dosage form design, AAPS PharmSciTech 13 (2012) 125–133.
[18] M.I. Alam, S. Baboota, A. Ahuja, M. Ali, J. Ali, J.K. Sahni, Intranasal infusion of nanostructured lipid carriers (NLC) containing CNS acting drug and estimation in brain and blood, Drug Deliv. 20 (2013) 247–251.
[19] S.Z.H. Rizvi, F.A. Shah, N. Khan, I. Muhammad, K.H. Ali, M.M. Ansari, Fu. Din, O.S. Qureshi, K.-W. Kim, Y.-H. Choe, J.-K. Kim, A. Zeb, Simvastatin-loaded solid lipid nanoparticles for enhanced anti-hyperlipidemic activity in hyperlipidemia animal model, Int. J. Pharm. 560 (2019) 136–143.
[20] R.H. Müller, K. Mäder, S. Gohla, Solid lipid nanoparticles (SLN) for controlled drug delivery – a review of the state of the art, Eur. J. Pharm. Biopharm. 50 (2000) 161–177.
[21] F.U. Din, W. Aman, I. Ullah, O.S. Qureshi, O. Mustapha, S. Shafique, A. Zeb, Effective use of nanocarriers as drug delivery systems for the treatment of selected tumors, Int. J. Nanomedicine 12 (2017) 7291–7309.
[22] C. Tapeinos, M. Battaglini, G. Ciofani, Advances in the design of solid lipid nanoparticles and nanostructured lipid carriers for targeting brain diseases, J. Control. Release 264 (2017) 306–332.
[23] O.S. Qureshi, H.S. Kim, A. Zeb, J.S. Choi, H.S. Kim, J.E. Kwon, M.S. Kim, J.H. Kang, C. Ryou, J.S. Park, J.K. Kim, Sustained release docetaxel-incorporated lipid nanoparticles with improved pharmacokinetics for oral and parenteral administration, J. Microencapsul. 34 (2017) 250–261.
[24] N. Khan, F.A. Shah, I. Rana, M.M. Ansari, Fu. Din, S.Z.H. Rizvi, W. Aman, G.-Y. Lee, E.-S. Lee, J.-K. Kim, A. Zeb, Nanostructured lipid carriers-mediated brain delivery of carbamazepine for improved in vivo anticonvulsant and anxiolytic activity, Int. J. Pharm. 577 (2020) 119033.
[25] A. Zeb, O.S. Qureshi, H.-S. Kim, M.-S. Kim, J.-H. Kang, J.-S. Park, J.-K. Kim, High payload itraconazole-incorporated lipid nanoparticles with modulated release property for oral and parenteral administration, J. Pharm. Pharmacol. 69 (2017) 955–966.
[26] R. Dang, X. Zhou, M. Tang, P. Xu, X. Gong, Y. Liu, H. Jiao, P. Jiang, Fish oil supplementation attenuates neuroinflammation and alleviates depressive-like behavior in rats submitted to repeated lipopolysaccharide, Eur. J. Nutr. 57 (2018) 893–906.
[27] A. Rex, R. Schickert, H. Fink, Antidepressant-like effect of nicotinamide adenine dinucleotide in the forced swim test in rats, Pharmacol. Biochem. Behav. 77 (2004) 303–307.
[28] A. Can, D.T. Dao, C.E. Terrillion, S.C. Piantadosi, S. Bhat, T.D. Gould, The tail suspension test, J. Vis. Exp. (2012) e3769-e3769.
[29] F.A. Shah, A. Zeb, T. Ali, T. Muhammad, M. Faheem, S.I. Alam, K. Saeed, P.O. Koh, K.W. Lee, M.O. Kim, Identification of proteins differentially expressed in the striatum by melatonin in a middle cerebral artery occlusion rat model-a proteomic and in silico approach, Front. Neurosci. 12 (2018) 888.
[30] R.J. Mumper, Z. Cui, M.O. Oyewumi, Nanotemplate engineering of cell specific nanoparticles, J. Dispers. Sci. Technol. 24 (2003) 569–588.
[31] T. Schmidts, D. Dobler, C. Nissing, F. Runkel, Influence of hydrophilic surfactants on the properties of multiple W/O/W emulsions, J. Colloid Interface Sci. 338 (2009) 184–192.
[32] A.B. Etame, C.A. Smith, W.C.W. Chan, J.T. Rutka, Design and potential application of PEGylated gold nanoparticles with size-dependent permeation through brain microvasculature, Nanomedicine 7 (2011) 992–1000.
[33] C. Saraiva, C. Praça, R. Ferreira, T. Santos, L. Ferreira, L. Bernardino, Nanoparticle-mediated brain drug delivery: overcoming blood–brain barrier to treat neurodegenerative diseases, J. Control. Release 235 (2016) 34–47.
[34] P.R. Lockman, J.M. Koziara, R.J. Mumper, D.D. Allen, Nanoparticle surface charges alter blood-brain barrier integrity and permeability, J. Drug Target. 12 (2004) 635–641.
[35] M.D. Howard, X. Lu, J.J. Rinehart, M. Jay, T.D. Dziubla, Physicochemical characterization of nanotemplate engineered solid lipid nanoparticles, Langmuir 27 (2011) 1964–1971.
[36] S. Gao, D.J. McClements, Formation and stability of solid lipid nanoparticles fabricated using phase inversion temperature method, Colloids Surf. A Physicochem. Eng. Asp. 499 (2016) 79–87.
[37] P. Severino, S.C. Pinho, E.B. Souto, M.H.A. Santana, Polymorphism, crystallinity and hydrophilic–lipophilic balance of stearic acid and stearic acid–capric/caprylic triglyceride matrices for production of stable nanoparticles, Colloids Surf. B Biointerfaces 86 (2011) 125–130.
[38] P.A. Makoni, K. Wa Kasongo, R.B. Walker, Short term stability testing of efavirenz-loaded solid lipid nanoparticle (SLN) and nanostructured lipid carrier (NLC) dispersions, Pharmaceutics 11 (2019) 397.
[39] C. Freitas, R.H. Müller, Effect of light and temperature on zeta potential and physical stability in solid lipid nanoparticle (SLN™) dispersions, Int. J. Pharm. 168 (1998) 221–229.
[40] D. Hou, C. Xie, K. Huang, C. Zhu, The production and characteristics of solid lipid nanoparticles (SLNs), Biomaterials 24 (2003) 1781–1785.
[41] A. zur Mühlen, C. Schwarz, W. Mehnert, Solid lipid nanoparticles (SLN) for controlled drug delivery – drug release and release mechanism, Eur. J. Pharm. Biopharm. 45 (1998) 149–155.
[42] P.R. Ravi, N. Aditya, H. Kathuria, S. Malekar, R. Vats, Lipid nanoparticles for oral delivery of raloxifene: optimization, stability, in vivo evaluation and uptake mechanism, Eur. J. Pharm. Biopharm. 87 (2014) 114–124.
[43] O.S. Qureshi, A. Zeb, M. Akram, M.-S. Kim, J.-H. Kang, H.-S. Kim, A. Majid, I. Han, S.-Y. Chang, O.-N. Bae, J.-K. Kim, Enhanced acute anti-inflammatory effects of CORM-2-loaded nanoparticles via sustained carbon monoxide delivery, Eur. J. Pharm. Biopharm. 108 (2016) 187–195.
[44] R. Yankelevitch-Yahav, M. Franko, A. Huly, R. Doron, The forced swim test as a model of depressive-like behavior, J. Vis. Exp. (2015) 52587.
[45] C. Mannari, N. Origlia, A. Scatena, A. Del Debbio, M. Catena, G. Dell'agnello, A. Barraco, L. Giovannini, L. Dell'osso, L. Domenici, A. Piccinni, BDNF level in the rat prefrontal cortex increases following chronic but not acute treatment with duloxetine, a dual acting inhibitor of noradrenaline and serotonin re-uptake, Cell. Mol. Neurobiol. 28 (2008) 457–468.
[46] M. Molnar, S.G. Potkin, W.E. Bunney Jr, E.G. Jones, MRNA expression patterns and distribution of white matter neurons in dorsolateral prefrontal cortex of depressed patients differ from those in schizophrenia patients, Biol. Psychiatry 53 (2003) 39–47.
[47] F. Karege, G. Perret, G. Bondolfi, M. Schwald, G. Bertschy, J.-M. Aubry, Decreased serum brain-derived neurotrophic factor levels in major depressed patients, Psychiatry Res. 109 (2002) 143–148.
[48] A.B. Klein, R. Williamson, M.A. Santini, C. Clemmensen, A. Ettrup, M. Rios,

G.M. Knudsen, S. Aznar, Blood BDNF concentrations reflect brain-tissue BDNF levels across species, Int. J. Neuropsychopharmacol. 14 (2011) 347–353.
[49] S.W. Jeon, Y.K. Kim, Neuroinflammation and cytokine abnormality in major depression: Cause or consequence in that illness? World J. Psychiatry 6 (2016) 283–293.
[50] K.L. Wu, S.H. Chan, J.Y. Chan, Neuroinflammation and oxidative stress in rostral ventrolateral medulla contribute to neurogenic hypertension induced by systemic inflammation, J. Neuroinflamm. 9 (2012) 212.
[51] T. Ali, S.U. Rahman, Q. Hao, W. Li, Z. Liu, F. Ali Shah, I. Murtaza, Z. Zhang, X. Yang, G. Liu, S. Li, Melatonin prevents neuroinflammation and relieves depression by attenuating autophagy impairment through FOXO3a regulation, J. Pineal Res. (2020).
[52] M.L. Wong, A. Inserra, M.D. Lewis, C.A. Mastronardi, L. Leong, J. Choo, S. Kentish, P. Xie, M. Morrison, S.L. Wesselingh, G.B. Rogers, J. Licinio, Inflammasome signaling affects anxiety- and depressive-like behavior and gut microbiome composition, Mol. Psychiatry 21 (2016) 797–805.
[53] C.L. Raison, L. Capuron, A.H. Miller, Cytokines sing the blues: inflammation and the pathogenesis of depression, Trends Immunol. 27 (2006) 24–31.
[54] Y. Liu, R.C. Ho, A. Mak, Interleukin (IL)-6, tumour necrosis factor alpha (TNF-alpha) and soluble interleukin-2 receptors (sIL-2R) are elevated in patients with major depressive disorder: a meta-analysis and meta-regression, J. Affect. Disord. 139 (2012) 230–239.
[55] Q. Chen, Y. Luo, S. Kuang, Y. Yang, X. Tian, J. Ma, S. Mai, L. Xue, J. Yang, Cyclooxygenase-2 signalling pathway in the cortex is involved in the pathophysiological mechanisms in the rat model of depression, Sci. Rep. 7 (2017) 488-488.
[56] D. Liu, Z. Wang, S. Liu, F. Wang, S. Zhao, A. Hao, Anti-inflammatory effects of fluoxetine in lipopolysaccharide(LPS)-stimulated microglial cells, Neuropharmacology 61 (2011) 592–599.
[57] X. Dong, Current strategies for brain drug delivery, Theranostics 8 (2018) 1481–1493.
[58] A. Zeb, J.-H. Cha, A.R. Noh, O.S. Qureshi, K.-W. Kim, Y.-H. Choe, D. Shin, F.A. Shah, A. Majid, O.-N. Bae, J.-K. Kim, Neuroprotective effects of carnosine-loaded elastic liposomes in cerebral ischemia rat model, J. Pharm. Investig. (2019).
[59] W.M. Lim, P.S. Rajinikanth, C. Mallikarjun, Y.B. Kang, Formulation and delivery of itraconazole to the brain using a nanolipid carrier system, Int. J. Nanomedicine 9 (2014) 2117–2126.
[60] P. Blasi, S. Giovagnoli, A. Schoubben, M. Ricci, C. Rossi, Solid lipid nanoparticles for targeted brain drug delivery, Adv. Drug Deliv. Rev. 59 (2007) 454–477.